Preprints, Fourth IFAC Conference on
Modelling, Identification and Control of Nonlinear Systems
Lyon, France. September 4-6, 2024

Maximum-likelihood arrival cost for moving-horizon estimation – Application to mammalian cell culture

Fernando N. Santos-Navarro * **Guilherme A. Pimentel** *
Laurent Dewasme * **Alain Vande Wouwer** *

* *Systems, Estimation, Control and Optimization (SECO) ,
University of Mons, 7000 Mons, Belgium
(e-mail: {fernandonobel.santosnavarro, guilherme.araujopimentel,
laurent.dewasme, alain.vandewouwer}@umons.ac.be).*

Abstract: Moving-horizon estimation performance depends on the arrival-cost approximation. Different methods exist to approximate the arrival cost with different trade-offs, such as limited performance, complex implementation, or abusive computational cost. In particular, we can distinguish two different methods based on using an external filter or the optimality conditions to calculate the covariance of the estimations. This paper presents a simpler alternative for the arrival-cost approximation based on maximum-likelihood estimation. The performance of this approximation is assessed using a mammalian cell culture case study where biomass and glutamine concentrations are estimated.

Keywords: Nonlinear observer, Moving-horizon estimation, Arrival-cost approximation, Industrial biotechnology

1. INTRODUCTION

The pharmaceutical industry commonly uses mammalian cell cultures to produce metabolites and proteins of interest (Farzan et al., 2017). The operation of this bioprocess depends on knowledge of key variables such as the concentration of viable cell biomass or critical substrates such as glutamine. However, viable biomass and glutamine online measurements are often achieved by expensive probes, may remain inaccurate, and require time-consuming calibrations. Observers or soft-sensors constitute a promising alternative for inferring non-measurable or difficult-to-measure variables from other available metabolite measurements. Throughout the scientific literature, many observers with different properties and computational costs have been designed to solve this estimation problem, such as the asymptotic observer (Bastin and Dochain, 1990) or the Kalman filter (Dubach and Märkl, 1992; Su et al., 2003; Ohadi et al., 2015). Thanks to the increased computational power of modern computers, optimization-based observers, such as full-horizon estimators (FHE) (Bogaerts and Hanus, 2001), can be used online. However, the computational cost of full-horizon estimation can still be prohibitive in many applications. Therefore, moving-horizon estimation (MHE) has been developed (Rao et al., 2001; Alamir and Corriou, 2002; Goffaux and Vande Wouwer, 2008), which offers almost comparable performance as full-horizon estimation but at a lower computational cost.

The performance of the moving horizon estimator is tightly related to the accuracy of the arrival cost approximation. The arrival cost incorporates information from past measurements, which are no longer considered, into the current finite window of the moving-horizon estimator to reproduce the level of information of the full-horizon version. Different methods exist to approximate the arrival cost, with different trade-offs such as limited performance (related to the ability to mimic the full-horizon estimator, to recover from imprecise initial conditions and covariances, to guarantee stability), complex implementation, and abusive computational cost. In particular, we can distinguish two different approaches to calculate the arrival cost based on: (i) the use of an external filter (Robertson et al., 1996; Rao and Rawlings, 2002) and (ii) the use of optimality conditions (López-Negrete and Biegler, 2012; Bansal et al., 2016). The first approach considers an external filter, such as the extended Kalman filter (EKF), to calculate the covariance of the estimation and approximate the arrival cost. However, this approach adds extra complexity to the formulation and implementation of the moving-horizon estimator. The second approach uses the inverse of the Hessian of the cost function at the optimum as an approximation of the covariance and the arrival cost. This approach avoids the extra complexity of the external filter approach, and it has no loss in performance (Elsheikh et al., 2021). However, the root problem is that, in both approaches, the formulation of the moving-horizon estimator only provides the estimation of the state without the covariance, requiring exogenous forms of arrival cost calculations.

In this paper, we propose an MHE formulation based on maximum-likelihood estimation that provides both mean and covariance estimation of the states. This formulation combines the work of Bogaerts and Hanus (2001) and Alamir (2007), and the main contribution is the addition of the arrival-cost approximation based on maximum likelihood. The aim of this paper is to propose this MHE

formulation and validate it with an experimental case of mammalian cell cultures.

The paper is organized as follows. Section 2 describes the moving-horizon estimation formulation based on maximum likelihood and its corresponding arrival cost approximation. Section 3 presents the experimental case study. Finally, Section 4 concludes the paper and points out future work.

2. MOVING HORIZON ESTIMATION

2.1 Definition of the system to estimate

A nonlinear system of the following form is considered:

$$\dot{x}(t) = f(t, x(t)) \tag{1}$$
$$y(t) = h(t, x(t)) + v(t) \tag{2}$$

where $x(t) \in \mathbb{R}^n$ is the state vector, $y(t) \in \mathbb{R}^{n_y}$ is the measurement vector, $f(t, x(t))$ and $h(t, x(t))$ are nonlinear functions describing, respectively, the system and measurement output dynamics, and $v(t) \in \mathbb{R}^{n_y}$ is the measurement noise vector which is assumed to have a Gaussian distribution with zero mean and a covariance matrix $R(t)$. Note that the dependence on known variables (e.g., the control action or time-varying parameters) is handled implicitly through the argument t in $f(t, x(t))$ and $h(t, x(t))$.

We define:

$$X(t, t_0, x_0) := x(t) \tag{3}$$
$$Y(t, t_0, x_0) := h(t, x(t)) \tag{4}$$

where $X : \mathbb{R}_+ \times \mathbb{R}_+ \times \mathbb{R}^n \to \mathbb{R}^n$ and $Y : \mathbb{R}_+ \times \mathbb{R}_+ \times \mathbb{R}^n \to \mathbb{R}^{n_y}$ are maps which give, respectively, the value of state $x(t)$ and the measurement function $h(t, x(t))$ at the time instant t based on the knowledge of the state $x(t_0) = x_0$ in some instant t_0.

Finally, we assume that $\mathcal{X}(t)$ is a known map that gives the set of admissible state values such that the following inclusion is satisfied at each instant t:

$$x(t) \in \mathcal{X}(t) \subset \mathbb{R}^n. \tag{5}$$

2.2 Moving-horizon estimation formulation

Once we have defined the equations of the system to be estimated, we define the MHE formulation as follows: (i) we define how to handle the window size, (ii) we define the cost function to be minimized, (iii) we define how the covariance is calculated using maximum-likelihood and (iv), finally, how the arrival cost is approximated.

The moving-horizon estimator considers a window of size N that covers the most recent $N + 1$ measurements. The start-up, therefore, requires to reach $N + 1$ measurements or, instead, to run a full-horizon estimator using all available measurements during the start-up period. The second proposition is preferred and Figure 1 proposes a conceptual view of the transition from FHE to MHE.

For the sake of simplicity, FHE and MHE are defined under the same generic formulation where a window covers all measurements from k_0 to k. In this way, k_0 can be considered as the batch initial time for the FHE ($k_0 = 0$)

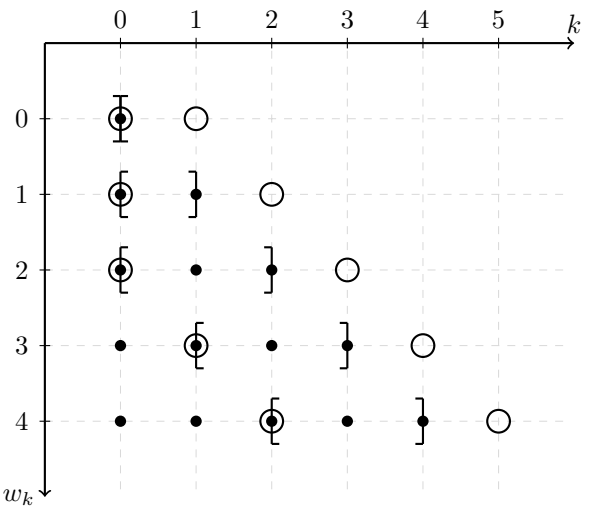

Fig. 1. Representation of the windows of a moving-horizon estimator with window size $N = 2$. The x-axis is the time k and the y-axis is the window w_k at time k. The dots are all the available measurements at time k, the square brackets define the measurements inside the current window w_k, and the circles are the *a priori* knowledge of the states at time k ($\bar{x}_k$ and $\bar{Q}_k$) using the past measurements.

or the window initial time for the MHE ($k_0 = k - N$), as follows:

$$k_0 = \begin{cases} 0, & \text{if } \ k \leqslant N \\ k - N, & \text{if } \ k > N \end{cases}. \tag{6}$$

For the system from Section 2.1, we define an MHE updated at instants $t_k = k\tau_s$, as follows:

$$\hat{x}(t) = X(t, t_{k_0}, \hat{x}_{k_0|k}) \quad \forall t \in [t_k, t_{k+1}[\tag{7}$$
$$\hat{x}_{k_0|k} = \underset{x_{k_0} \in \mathcal{X}(t_{k_0})}{\arg\min} \ J^k_{k_0}(x_{k_0}) \tag{8}$$

where $\hat{x}(t)$ is the state prediction for the time interval $[t_k, t_{k+1}[$, $\hat{x}_{k_0|k}$ is the most-likely state estimation for the instant t_{k_0} using all the information available at time t_k, and $J^k_{k_0}(x_{k_0})$ is the following cost function:

$$J^k_{k_0}(x_{k_0}) = ||\bar{x}_{k_0} - x_{k_0}||^2_{\bar{Q}_{k_0}} + \sum_{i=k_0}^{k} ||y(t_i) - Y(t_i, t_{k_0}, x_{k_0})||^2_{R(t_i)} \tag{9}$$

where $\bar{x}_{k_0}$ is an *a priori* estimation of the state at time t_{k_0} and $\bar{Q}_{k_0}$ is the covariance matrix of $\bar{x}_{k_0}$.

Note that (i) it is assumed that all measurements are sampled with the same sampling rate τ_s, but this can be easily adapted in a multi-rate scenario, and (ii) the system equations are never discretized, $X(t, t_{k_0}, \hat{x}_{k_0|k})$ is a continuous simulation of the system dynamics.

2.3 Confidence interval calculation

We can approximate the confidence interval of the FHE and MHE estimates by extending the procedure described in Bogaerts and Hanus (2001) to take into account the maximum-likelihood arrival cost ($\bar{x}_{k_0}$ and $\bar{Q}_{k_0}$). The covariance matrix of the estimated state at the beginning of a window, $Q_{k_0|k}$, can be approximated as:

$$Q_{k_0|k} \approx \left(\bar{Q}_{k_0}^{-1} + \sum_{i=k_0}^{k} ||C(t_i, t_{k_0}, \hat{x}_{k_0|k}) G(t_i, t_{k_0}, \hat{x}_{k_0|k})||^2_{R(t_i)}\right)^{-1} \tag{10}$$

where $C(t, t_0, x_0)$ is the Jacobian of the measurement function at time t using similar notation as $X(t, t_0, x_0)$:

$$C(t, t_0, x_0) := \left.\frac{\partial h(t, x)}{\partial x}\right|_{x=x_0} \tag{11}$$

and $G(t, t_0, x_0)$ is the sensitivity of the state at instant t with respect the initial state x_0:

$$G(t, t_0, x_0) := \left.\frac{\partial X(t, t_0, x)}{\partial x}\right|_{x=x_0} \tag{12}$$

which can be calculated numerically by solving the following differential equation:

$$\frac{\partial}{\partial t} G(t, t_0, x_0) = \frac{\partial f(t, x)}{\partial x} G(t, t_0, x_0) \tag{13}$$

with the initial condition:

$$G(t_0, t_0, x_0) = I_n. \tag{14}$$

Then we can approximate the value of the covariance of $\hat{x}(t)$ for the time interval $[t_k, t_{k+1}[$ as:

$$\begin{aligned} Q(t) \approx\ & G(t, t_{k_0}, \hat{x}_{k_0|k}) \times Q_{k_0|k} \\ & \times G(t, t_{k_0}, \hat{x}_{k_0|k})^T \quad \forall t \in [t_k, t_{k+1}[. \end{aligned} \tag{15}$$

Finally, the confidence intervals can be inferred from the diagonal terms of $Q(t)$.

2.4 Maximum-likelihood arrival cost

The arrival cost ($\bar{x}_{k_0}$ and $\bar{Q}_{k_0}$) summarizes all the past measurements that are not considered in the current window.

For the time instants $k \leqslant N$ (FHE), the arrival cost is assumed to be known: it is just the *a priori* estimated initial condition $\bar{x}_0$ and its covariance matrix $\bar{Q}_0$.

For the time instants $k > N$ (MHE), the arrival cost is calculated from the solution of a previous window. For the window k we can calculate $\bar{x}_{k+1}$ and $\bar{Q}_{k+1}$ as:

$$\bar{x}_{k+1} = X(t_{k+1}, t_{k_0}, \hat{x}_{k_0|k}) \tag{16}$$

$$\begin{aligned} \bar{Q}_{k+1} = & G(t_{k+1}, t_{k_0}, \hat{x}_{k_0|k}) \times Q_{k_0|k} \\ & \times G(t_{k+1}, t_{k_0}, \hat{x}_{k_0|k})^T \end{aligned} \tag{17}$$

where $\bar{x}_{k+1}$ is the most-likely estimate for the state at time t_{k+1} using all the information available at time t_k and $\bar{Q}_{k+1}$ is the covariance of $\bar{x}_{k+1}$.

Then, the arrival cost of window k is calculated using the solution of the previous window $k - N - 1$.

2.5 Fixed-covariance arrival cost

In the following case study, we intend to test the ability of the MHE maximum-likelihood arrival cost to reproduce the performance of the equivalent FHE. We will compare those results with another way to compute the arrival cost: the fixed-covariance arrival cost. This method consists on using $\bar{x}_{k+1}$ as the maximum-likelihood approach (the solution of the window k integrated to time $k+1$), but the covariance matrix is set to a constant value:

$$\bar{Q}_{k+1} = I_n. \tag{18}$$

This fixed-covariance arrival cost will show that it is not enough to set $\bar{Q}_{k+1}$ to a fixed value for the MHE to imitate the FHE.

Then, for comparing the capability of both methods to replicate the full-horizon estimator, we define the sum of squared errors of the state estimation (SSE mean) and its standard deviation (SSE std.) of the MHE solution with respect to the FHE as:

$$\text{SSE mean} = \sum_{i=0}^{k} ||\hat{x}_{\text{FHE}}(t_i) - \hat{x}_{\text{MHE}}(t_i)||^2 \tag{19}$$

$$\text{SSE std} = \sum_{i=0}^{k} ||\hat{\sigma}_{\text{FHE}}(t_i) - \hat{\sigma}_{\text{MHE}}(t_i)||^2 \tag{20}$$

where k is the total length of the experiment, $\hat{x}_{\text{FHE}}(t_i)$ and $\hat{x}_{\text{MHE}}(t_i)$ are the state estimations of the full and moving horizon estimators, respectively, at time t_i, and $\hat{\sigma}_{\text{FHE}}(t_i)$ and $\hat{\sigma}_{\text{FHE}}(t_i)$ are the standard deviation of the estimations.

2.6 Implementation

The FHE and MHE algorithms presented in the previous sections were implemented in MATLAB R2020b. The FHE and MHE were converted into non-linear programming problems (NLP) using Runge-Kutta 4th and multiple-shooting. CasADi (Andersson et al., 2019) was used to define the NLP problems, and IPOPT (Wächter and Biegler, 2006) to solve them.

3. CASE STUDY: MAMMALIAN CELL CULTURES

The set-up of a full and moving horizon estimator is considered in the realistic context of mammalian cell cultures, where viable biomass and glutamine concentrations must be estimated from glucose and lactate concentration measurements.

3.1 Experimental data

The case study considered experimental data from Pimentel et al. (2023), which consists of a batch culture of HEK293-6E mammalian cells grown in a 200 mL T-flask with a predefined initial biomass concentration. The culture time is six days, and the concentrations of glucose, lactate, viable cells, and glutamine are measured off-line once a day. Figure 2 shows the experimental data with their corresponding confidence interval.

Table 1 shows (i) the standard deviation of the experimental data measurements and (ii) the selected initial condition (and its the standard deviation) used to initialize the estimators. The selected initial condition is an *a priori* estimate without using the biomass and glutamine measurements (because the observer cannot use these data in the real-world scenario). Therefore, this initial condition is not the most likely initial condition of the experiment; it is just the prior knowledge used to set up the observer. We could have set the initial condition to zero (with a large covariance), but using this *a priori* initial condition, we can (i) show how the observer recovers from an inaccurate initial condition and (ii) compare the observer's estimate with the model's prediction from that initial condition.

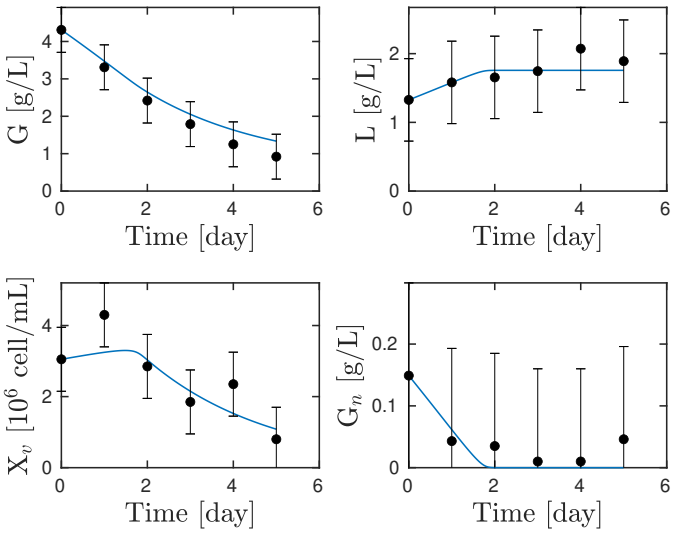

Fig. 2. Fitting of the macroscopic model (blue line) to the experimental data (black dots) of a batch culture of mammalian cells (Pimentel et al., 2023), where G is glucose, L is lactate, X is viable biomass and G_n is glutamine. All the confidence intervals are at 99%.

Table 1. (Measurement) Standard deviation of the experimental measurements, and (Initial condition) the value and standard deviation of the initial condition used to initialize the estimators (which is not the initial condition of the experiment).

State	Measurement	Initial condition		Units
	Std.	Value	Std.	
G	0.2	4.31	0.3	$\mathrm{g\,L^{-1}}$
L	0.2	1.3271	0.3	$\mathrm{g\,L^{-1}}$
X	0.3	1.0	1.0	$10^6\mathrm{cell\,L^{-1}}$
G_n	0.05	0.05	0.1	$\mathrm{g\,L^{-1}}$

3.2 Macroscopic model

The macroscopic model from Pimentel et al. (2023) describes the catabolism of the cells based on three bioreactions: (1) substrate oxidation (consumption of glucose and glutamine), (2) biomass death, and (3) viable biomass maintenance. The corresponding ordinary differential equation (ODE) system is obtained by mass balance application and reads:

$$\dot{G} = -k_{11}\varphi_1 - k_{13}\varphi_3 \tag{21}$$

$$\dot{L} = k_{21}\varphi_1 \tag{22}$$

$$\dot{X} = k_{31}\varphi_1 - k_{32}\varphi_2 \tag{23}$$

$$\dot{G}_n = -k_{41}\varphi_1 \tag{24}$$

with:

$$\varphi_1 = \mu_1 \frac{G}{K_{11}+G}\frac{G_n}{K_{41}+G_n}X \tag{25}$$

$$\varphi_2 = \mu_2 \frac{K_{42}}{K_{42}+G_n}X \tag{26}$$

$$\varphi_3 = \mu_3 \frac{G}{K_{13}+G}X \tag{27}$$

where G, L, X, and G_n are the concentrations of glucose, lactate, viable biomass, and glutamine, respectively. φ_j $(j = 1, 2, 3)$ is the j^{th} reaction rate and k_{ij} $(i = 1, 2, 3, 4)$ is the pseudo-stoichiometric coefficient of the i^{th} element of the j^{th} reaction. K_{ij} is the kinetic coefficient related to the factor of the i^{th} element in the j^{th} reaction rate and μ_j is the maximum constant of the j^{th} reaction rate. The model parameters are listed in Table 2, and K_{41}, K_{42} and K_{13} were set to small values to conserve model positiveness with negligible loss of data fitting.

Table 2. Mammalian cell culture model: parameter values

Parameter	Value	Units
k_{11}	0.4433	$\mathrm{g\,L^{-1}}$
k_{21}	1.016	$\mathrm{g\,L^{-1}}$
k_{31}	1	$10^6\mathrm{cell\,L^{-1}}$
k_{41}	0.3519	$\mathrm{g\,L^{-1}}$
k_{32}	1	$10^6\mathrm{cell\,L^{-1}}$
k_{13}	1	$\mathrm{g\,L^{-1}}$
μ_1	0.082 803	$\mathrm{day^{-1}}$
μ_2	0.3432	$\mathrm{day^{-1}}$
μ_3	0.2307	$\mathrm{day^{-1}}$
K_{11}	0.001	$\mathrm{g\,L^{-1}}$
K_{41}	0.005	$\mathrm{g\,L^{-1}}$
K_{42}	0.005	$\mathrm{g\,L^{-1}}$
K_{13}	0.0001	$\mathrm{g\,L^{-1}}$

Figure 2 shows that the macroscopic model fits the experimental data within the confidence intervals. However, the low sampling rate (one measurement per day) and the measurement noise make the observer implementation quite challenging. Even if this study aims to tackle the problem of state estimation with low measurement sampling, glucose, and lactate concentrations could be measured online at a faster rate using, for instance, devices such as the BioPAT®Trace from Sartorius (Abbate et al., 2020) reaching samplings of a couple of minutes. The system observability, considering the measurement configuration, has been checked and validated using the STRIKE GOLDD software (Villaverde et al., 2016). During the experiment, glutamine is almost depleted on day three, and the model predicts full depletion before the second day. Although estimating glutamine via glucose and lactate remains possible, it is important to note that the data starting at day 3 are inaccurate since glutamine can not be produced and the real concentration is probably below the sensitivity level of the analytical measurement device.

3.3 Results

Figure 3 shows the satisfactory performance of both FHE and MHE estimating biomass and glutamine. Also, it should be highlighted that the performance of both observers is almost equivalent: there are only minor differences in biomass estimation and its confidence interval.

The initial guess of the estimates was set far from the experimental data. However, both observers were able to recover from that inaccurate initial condition.

Figure 4 shows that the performance of the MHE and FHE is no longer equivalent when a fixed covariance arrival cost is used for the moving horizon estimation. Note that all the conditions in Figure 4 are the same as in Figure 3,

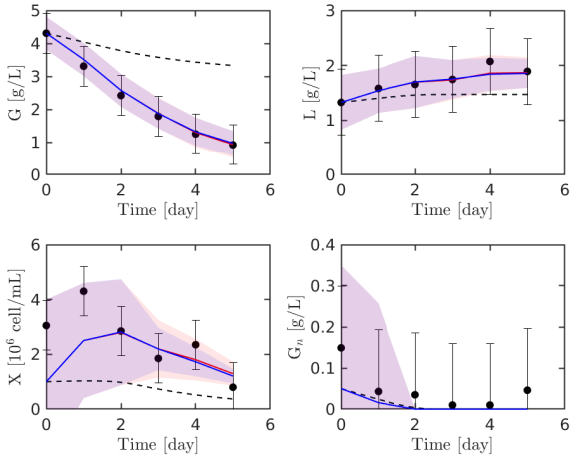

Fig. 3. Estimation of viable biomass X_v and glutamine G_n from glucose G and lactate L measurements by full and moving horizon estimation: experimental data (black dot), full horizon estimation (red line), its confidence interval (red area), moving horizon estimation with window size $N = 1$ (blue line), its confidence interval (blue area) and macroscopic model simulation (dashed line) starting from the same initial condition as the observers. All confidence intervals are at 99%.

except the way the arrival cost is calculated in the moving-horizon estimator. Until the first day, the performance of both observers is equivalent, since the MHE operates in the initial full-horizon mode. However, from the first day on, the performance of both observers starts differing.

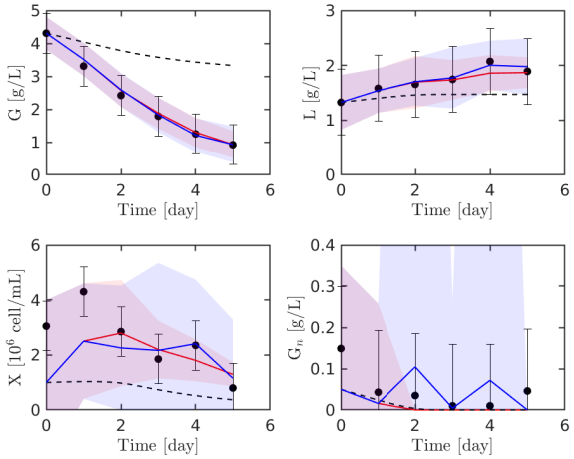

Fig. 4. Performance degradation of the moving horizon estimation when a fixed covariance arrival cost is used instead of the maximum likelihood covariance: experimental data (black dot), full horizon estimation (red line), its confidence interval (red area), moving horizon estimation with window size $N = 1$ and fixed covariance (blue line), its confidence interval (blue area) and model prediction (dashed line) starting from the same initial condition as the observers. All confidence intervals are at 99%.

Table 3 shows that the maximum likelihood-based arrival cost covariance calculation better replicates the full horizon results for any window size than the fixed covariance approach.

It should be noted how increasing the window size improves the performance of both methods. This results from two effects: as the window size increases, (i) more windows of the moving horizon estimation behave like the full-horizon estimator, and (ii) the arrival cost approximation is less relevant to the overall performance because there are more measurements in the window. Finally, with a window size $N = 5$, the performance of both moving horizon estimators becomes equivalent to the full horizon version since full data information is considered.

Table 3. Performance of moving-horizon estimation versus full-horizon estimation for different window sizes and different arrival cost covariance computations. The performance is measured as the sum of squared errors (SSE) between the solutions of the full and moving horizon estimations for the mean (SSE mean) and the standard deviation (SSE std.) of the estimations.

Window size	MHE maximum likelihood[1]		MHE fixed[2]	
	SSE mean	SSE std.	SSE mean	SSE std.
1	1.7×10^{-2}	1.8×10^{-2}	7.4×10^{-1}	2.9
2	2.2×10^{-2}	1.4×10^{-2}	4.1×10^{-1}	1.1
3	9.3×10^{-3}	3.6×10^{-3}	6.4×10^{-1}	4.9×10^{-1}
4	5.2×10^{-6}	7.2×10^{-6}	5.4×10^{-2}	2.9×10^{-2}
5	0	0	0	0

[1] Moving-horizon estimation using maximum-likelihood arrival-cost covariance.
[2] Moving-horizon estimation using fixed arrival-cost covariance.

In this case study, the maximum-likelihood arrival cost allows the moving-horizon estimator to reproduce the performance of the full-horizon version. However, if the distribution of the state estimation were multi-modal (Haseltine and Rawlings, 2005), then the maximum-likelihood approach would summarize it as a normal distribution, losing information in the process. Then, a loss in the performance of the moving-horizon estimator should be expected. However, this limitation is also the case with other approaches for calculating the arrival cost based on extended Kalman filters or optimality conditions.

The maximum likelihood method presented here can be classified as a filtering scheme (Haseltine and Rawlings, 2005). It is possible to define a smoothing-scheme arrival cost. The cost would be the extra complexity of handling the double-counting effect, but this could improve the performance of the observer (i.e., recovering from inaccurate initial conditions and covariances).

4. CONCLUSION

This paper proposes a maximum-likelihood arrival cost approximation that allows the moving-horizon estimator to reproduce the performance of the full-horizon estimator (under the conditions of this experimental case study).

Unlike the classical approximation of the arrival cost by external filters or optimality conditions, the implementation complexity of this estimator is reduced since the estimator already provides the estimate of the covariance, which is the basis for approximating the arrival cost. Both MHE and FHE were successfully validated in a real-life pharmaceutical application where mammalian cell biomass and glutamine are estimated.

Biomass estimation is a critical issue in bioprocess management. Improving the accessibility (both theoretical and practical) of the moving-horizon estimator can benefit the community, as it is a suitable and robust way to solve the underlying estimation problem.

ACKNOWLEDGEMENTS

The authors acknowledge the support of the ProtoDrive project (convention no. 2010119) of the Win2Wal program of the Walloon Region (DGO6) achieved in collaboration with the CER Groupe and Univercells Exothera. The scientific responsibility rests with its authors.

REFERENCES

Abbate, T., Sbarciog, M., Dewasme, L., and Vande Wouwer, A. (2020). Experimental validation of a cascade control strategy for continuously perfused animal cell cultures. *Processes*, 8, 413.

Alamir, M. (2007). *Nonlinear Moving Horizon Observers: Theory and Real-Time Implementation*, 139–179. Springer Berlin Heidelberg, Berlin, Heidelberg. doi:10.1007/978-3-540-73503-8_5.

Alamir, M. and Corriou, J.P. (2002). Nonlinear receding-horizon state estimation for dispersive adsorption columns with nonlinear isotherm. *Proceedings of the 41st IEEE Conference on Decision and Control, 2002.*, 2, 2334–2339 vol.2.

Andersson, J.A.E., Gillis, J., Horn, G., Rawlings, J.B., and Diehl, M. (2019). Casadi: a software framework for nonlinear optimization and optimal control. *Mathematical Programming Computation*, 11(1), 1–36. doi:10.1007/s12532-018-0139-4.

Bansal, A., Bhushan, M., and Biegler, L.T. (2016). Covariance computation in mhe: A nonlinear regression approach. In *2016 12th IEEE International Conference on Control and Automation (ICCA)*, 663–668. doi:10.1109/ICCA.2016.7505354.

Bastin, G. and Dochain, D. (1990). *On-line estimation and adaptive control of bioreactors*. Process measurement and control. Elsevier.

Bogaerts, P. and Hanus, R. (2001). On-line state estimation of bioprocesses with full horizon observers. *Mathematics and Computers in Simulation*, 56(4), 425–441. doi:https://doi.org/10.1016/S0378-4754(01)00312-3. Mathematical Modelling and Simulation in Agricultural and Bio-Industries.

Dubach, A.C. and Märkl, H. (1992). Application of an extended kalman filter method for monitoring high density cultivation of escherichia coli. *Journal of Fermentation and Bioengineering*, 73(5), 396–402. doi:https://doi.org/10.1016/0922-338X(92)90286-4.

Elsheikh, M., Hille, R., Tatulea-Codrean, A., and Krämer, S. (2021). A comparative review of multi-rate moving horizon estimation schemes for bioprocess applications. *Computers & Chemical Engineering*, 146, 107219. doi:https://doi.org/10.1016/j.compchemeng.2020.107219.

Farzan, P., Mistry, B., and Ierapetritou, M.G. (2017). Review of the important challenges and opportunities related to modeling of mammalian cell bioreactors. *AIChE Journal*, 63(2), 398–408. doi:https://doi.org/10.1002/aic.15442.

Goffaux, G. and Vande Wouwer, A. (2008). Design of a robust nonlinear receding-horizon observer - application to a biological system. *IFAC Proceedings Volumes*, 41(2), 15553–15558. doi:https://doi.org/10.3182/20080706-5-KR-1001.02630. 17th IFAC World Congress.

Haseltine, E.L. and Rawlings, J.B. (2005). Critical evaluation of extended kalman filtering and moving-horizon estimation. *Industrial & Engineering Chemistry Research*, 44(8), 2451–2460. doi:10.1021/ie034308l.

López-Negrete, R. and Biegler, L.T. (2012). A moving horizon estimator for processes with multi-rate measurements: A nonlinear programming sensitivity approach. *Journal of Process Control*, 22(4), 677–688. doi:https://doi.org/10.1016/j.jprocont.2012.01.013.

Ohadi, K., Legge, R., and Budman, H. (2015). Development of a soft-sensor based on multi-wavelength fluorescence spectroscopy and a dynamic metabolic model for monitoring mammalian cell cultures. *Biotechnology and Bioengineering*, 112. doi:10.1002/bit.25339.

Pimentel, G.A., Dewasme, L., Santos-Navarro, F.N., Boes, A., Côte, F., Filée, P., and Vande Wouwer, A. (2023). Macroscopic dynamic modeling of metabolic shift to lactate consumption of mammalian cell batch cultures. In *2023 9th International Conference on Control, Decision and Information Technologies (CoDIT)*, 1–6. doi:10.1109/CoDIT58514.2023.10284210.

Rao, C.V. and Rawlings, J.B. (2002). Constrained process monitoring: Moving-horizon approach. *AIChE Journal*, 48(1), 97–109. doi:https://doi.org/10.1002/aic.690480111.

Rao, C.V., Rawlings, J.B., and Lee, J.H. (2001). Constrained linear state estimation—a moving horizon approach. *Automatica*, 37(10), 1619–1628. doi:https://doi.org/10.1016/S0005-1098(01)00115-7.

Robertson, D.G., Lee, J.H., and Rawlings, J.B. (1996). A moving horizon-based approach for least-squares estimation. *AIChE Journal*, 42(8), 2209–2224. doi:https://doi.org/10.1002/aic.690420811.

Su, W.W., Li, J., and Xu, N.S. (2003). State and parameter estimation of microalgal photobioreactor cultures based on local irradiance measurement. *Journal of Biotechnology*, 105(1), 165–178. doi:https://doi.org/10.1016/S0168-1656(03)00188-3.

Villaverde, A.F., Barreiro, A., and Papachristodoulou, A. (2016). Structural identifiability of dynamic systems biology models. *PLOS Computational Biology*, 12(10), 1–22. doi:10.1371/journal.pcbi.1005153.

Wächter, A. and Biegler, L.T. (2006). On the implementation of an interior-point filter line-search algorithm for large-scale nonlinear programming. *Mathematical Programming*, 106(1), 25–57. doi:10.1007/s10107-004-0559-y.